

Three Phase Two Leg Neutral Point Clamped Converter with output DC Voltage Regulation and Input Power Factor Correction

B. Sirisha, N. Susheela, P. Satishkumar

Department of Electrical Engineering, Osmania University, Hyderabad
e-mail:sirishab2007@yahoo.com, satish_8020@yahoo.co.in, nsusheela2007@yahoo.com

Article Info

Article history:

Received Jan 15th, 2012

Revised Apr 17th, 2012

Accepted Apr 27th, 2012

Keyword:

neutral point clamped converter,
space vector modulation,
power factor

ABSTRACT

A three-phase neutral point clamped (NPC) converter is presented for power factor correction and dc-link voltage regulation. The adopted converter has simpler circuit configuration compared to three level PWM converters. A simplified space vector pulse width modulation scheme (SVPWM) is adopted to track line current commands. Using a simplified SVPWM algorithm, the calculate time for the time duration of voltage vector is reduced. The adopted NPC converter has less power switches compared with the conventional three-level NPC converter. Only eight power switches and four clamping diodes with voltage stress of half the dc bus voltage are used in the circuit configuration. Based on the proposed control algorithm, a reference voltage vector is generated on the ac terminal for drawing the sinusoidal line currents with unity power factor. Computer simulation results based on MATLAB/SIMULINK are presented to verify the validity and effectiveness of the proposed control strategy.

*Copyright © 2012 Institute of Advanced Engineering and Science.
All rights reserved.*

Corresponding Author:

Dr. P.Satishkumar,

Department of Electrical Engineering,

Osmania University, Hyderabad

Email: satish_8020@yahoo.co.in

1. INTRODUCTION

Diode or phase-controlled rectifiers are widely utilized in the front-end converter for the uncontrollable or controllable DC-bus voltage in industrial and commercial applications. However, low power factor and non sinusoidal line currents are drawn from the AC source owing to a large electrolytic capacitor used on the DC link. Power pollutants such as reactive power and current harmonics result in line-voltage distortion, heating of the transformer core and electrical machines, and increased losses in the transmission and distribution line. To meet the relevant standards in Europe and America, several current wave-shaping solutions have been proposed to achieve power factor correction and current-harmonic reduction. Multilevel rectifiers and inverters have been proposed for high power and medium-voltage applications because they provide advantages such as the low voltage rating of power semiconductors and low voltage harmonics. However, the disadvantages of the multilevel rectifiers are the large number of power semiconductors in the circuit, a complex control scheme and the neutral-point voltage balance problem. In industrial applications with a unidirectional power flow, conventional multilevel converters are too expensive and complicated to implement. A three-phase three-level AC/DC converter with fewer power switches is presented to achieve almost unity power factor, to regulate the DC-link voltage and to achieve fast dynamic response. The circuit topologies of multilevel inverters can be classified into neutral point diode clamped (NPC) inverters [12–13], flying capacitor clamped inverters [14–15], and cascade full bridge inverters. Three-phase three-level NPC converters were proposed in [18–20] to draw the sinusoidal line currents in phase with mains voltages. The input power factor is close to unity. However, twelve power switches and six clamping diodes are used in the circuit configuration.

2. PROPOSED EIGHT SWITCH NPC CONVERTER

Fig.1 shows the circuit configuration of the adopted three-phase NPC converter. Two NPC legs are used in the converter. Each NPC leg has four power semiconductor switches and two clamping diodes. Each power semiconductor has a voltage rating of half the dc bus voltage. Three boost inductors are connected to converter on the ac terminal. These inductors are used to achieve boost operation and to achieve line current filtering. The phase C is directly connected to the midpoint of the split dc capacitors. Three valid voltage levels are generated on the ac terminal voltages V_{ac} and V_{bc} . Five voltage levels are generated on the voltage V_{ab} based on the proper operation of two NPC legs. A dc bus voltage controller is used to balance the power demand between the ac source and dc load. A current controller is used to obtain the reference control voltage vector of the converter. The simplified space vector modulation is adopted to obtain the time duration of the selected voltage vectors. The time intervals of power switches corresponding to the selected voltage vectors are calculated to drive the converter. The control goals of the proposed converter are to obtain a constant dc-link voltage, to draw the sinusoidal line currents, and to achieve unity input power factor.

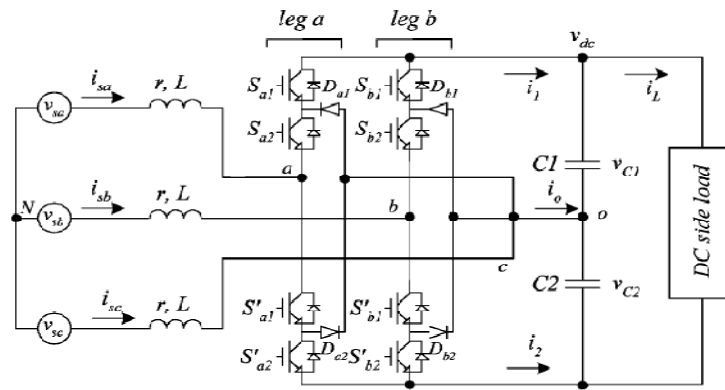


Figure 1: Proposed three phase two leg converter

A balanced three-phase three-line ac source is used in the adopted system. The sum of the instantaneous three-phase voltages and currents is zero

$$x_{sa} + x_{sb} + x_{sc} = 0 \quad (1)$$

Where x can be phase voltage or line current. The three-phase voltages and currents in the steady state are expressed as

$$\begin{aligned} v_{sa} &= V_{sm} \cos(\omega t) \\ v_{sb} &= V_{sm} \cos(\omega t - 2\pi/3) \\ v_{sc} &= V_{sm} \cos(\omega t + 2\pi/3) \end{aligned} \quad (2)$$

$$\begin{aligned} i_{sa} &= I_{sm} \cos(\omega t) \\ i_{sb} &= I_{sm} \cos(\omega t - 2\pi/3) \\ i_{sc} &= I_{sm} \cos(\omega t + 2\pi/3) \end{aligned} \quad (3)$$

Where V_{sm} and I_{sm} are the peak source and peak current of three-phase ac source, respectively, ϕ is the phase angle between the source voltage and line current. From the voltage equations on the ac terminal of the converter shown in Fig. 1, we have

$$\begin{aligned}
L \frac{di_{sa}}{dt} &= V_{sa} - ri_{sa} - V_{aN} \\
L \frac{di_{sb}}{dt} &= V_{sb} - ri_{sb} - V_{bN} \\
L \frac{di_{sc}}{dt} &= V_{sc} - ri_{sc} - V_{cN}
\end{aligned} \tag{4}$$

In the steady state, the reference control voltages in the stationary reference frame can be calculated from (2)–(4) for the given source voltages and the obtained line currents from the output of the control loop. The differential equation of (4) can be rewritten in the orthogonal coordinate and expressed as

$$L \frac{dI_s}{dt} = V_s - rI_s - V \tag{5}$$

Where

$$I_s = \begin{pmatrix} i_{s\alpha} \\ i_{s\beta} \end{pmatrix} = C \begin{pmatrix} i_{sa} \\ i_{sb} \\ i_{sc} \end{pmatrix}, V_s = \begin{pmatrix} v_{s\alpha} \\ v_{s\beta} \end{pmatrix} = C \begin{pmatrix} v_{sa} \\ v_{sb} \\ v_{sc} \end{pmatrix}, V = \begin{pmatrix} v_{\alpha} \\ v_{\beta} \end{pmatrix} = C \begin{pmatrix} v_{aN} \\ v_{bN} \\ v_{cN} \end{pmatrix} \tag{6}$$

For a unity power factor operation, the phase angle α between the line current and phase voltage is zero. Fig. 2 shows the phasor diagram of the converter for unity power factor operation. For the rectifier operation, the line current is in phase with phase voltage. There is a phase lag between the source voltage V_s and reference control voltage V . The magnitude and phase angle of the reference control voltage V can be calculated from (6) and expressed as

$$|V| = \sqrt{v_{\alpha}^2 + v_{\beta}^2}, \theta = \tan^{-1} \frac{v_{\beta}}{v_{\alpha}} \tag{7}$$

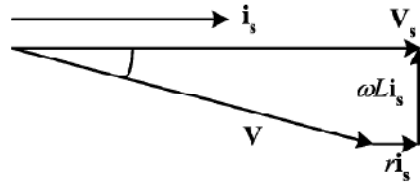


Figure 2: Phasor diagram of the converter for unity power factor operation

With the generated voltage vector in (7) on the ac terminal, the line currents are controlled to be sinusoidal waves with nearly unity power factor. However, the calculation time of trigonometric function and square root operation is too long. The high performance of digital controller is needed to obtain the reference voltage vector.

For the adopted three-phase NPC converter, eight power switches, and four clamping diodes are used.

The power switches S_{xy} and S_{xy}^1 ($x = a, b$; $y = 1, 2$) are complementary to each other to avoid the short circuit in each converter leg. Three valid switching states are available in each converter leg to achieve three voltage levels $v_{dc}/2$, 0 , $-v_{dc}/2$ on the ac terminal. For example of converter leg a, the upper two power switches S_{a1} and S_{a2} are closed to achieve voltage $V_{a0} = V_{ac} = v_{dc}/2$. In this operation state, line current i_{sa} is decreasing because $v_{sac} = v_{sa} - v_{sc} < v_{dc}/2$. If the power switches S_{a1}^1 and S_{a2}^1 are closed to turn on, the ac side voltage v_{ac} equals $-v_{dc}/2$. For this operation state, line current i_{sa} is increasing because $v_{sac} = v_{sa} - v_{sc} > -v_{dc}/2$. A zero voltage level is generated on the voltage v_{ac} if the middle two switches S_{a1}^1 and S_{a2}^1 are closed. For this operation condition, the phase current i_{sa} is increasing (or decreasing) if the line voltage v_{sac} is positive (or negative). Based on the above descriptions of three operation states in each converter leg, there are nine possible switching combinations in the adopted converter to control the line currents.

The voltages measured on the ac terminals depend on the states of power switches and can be expressed as

$$v_{aN} = v_{ao} + v_{oN} = f_a \frac{v_{dc}}{2} + v_{oN} \quad (8)$$

$$v_{abN} = v_{bo} + v_{oN} = f_b \frac{v_{dc}}{2} + v_{oN} \quad (9)$$

$$v_{cN} = v_{oN} \quad (10)$$

where v_{oN} is the voltage between the dc bus midpoint o and the point N on the ac source, and f_a and f_b are defined as

$$f_a = \begin{cases} 1, & \text{if } S_{a1} \text{ and } S_{a2} \text{ are closed} \\ 0, & \text{if } S'_{a1} \text{ and } S_{a2} \text{ are closed} \\ -1, & \text{if } S'_{a1} \text{ and } S'_{a2} \text{ are closed} \end{cases} \quad (11)$$

$$f_b = \begin{cases} 1, & \text{if } S_{b1} \text{ and } S_{b2} \text{ are closed} \\ 0, & \text{if } S'_{b1} \text{ and } S_{b2} \text{ are closed} \\ -1, & \text{if } S'_{b1} \text{ and } S'_{b1} \text{ are closed} \end{cases}$$

Applying (6) into (8)–(10), the ac terminal voltages in the orthogonal coordinate system are given by

$$v_\alpha = \frac{1}{\sqrt{6}} \left(f_a - \frac{f_b}{2} \right) v_{dc}, \quad v_\beta = \frac{1}{2\sqrt{2}} f_b v_{dc} \quad (12)$$

Based on the combinations of the switching states of switches, there are nine valid voltage vectors. The switching combinations can be represented by the order sets $[S_{a1}, S_{a2}, S_{b1}, S_{b2}]$, where $S_{a1} = 1$ denotes that power switch S_{a1} is closed, and $S_{a1} = 0$ denotes that power switch S_{a1} is open. The same notation applied to power switches S_{a2} , S_{b1} , and S_{b2} . The reference control voltages V_α and V_β in the orthogonal coordinate can be obtained from the ac terminal voltages v_{ac} and v_{bc} in the abc coordinate system by applying (12). These voltage vectors are given by

TABLE 1: THE OPERATION STATES AND CORRESPONDING SPACE VECTORS OF THE PROPOSED CONVERTER

vector	$(S_{a1}, S_{a2}, S_{b1}, S_{b2})$	v_α	v_β	V
V_0	$[0,1,0,1]$	0	0	$0\angle 0$
V_1	$[1,1,0,1]$	$\frac{v_{dc}}{\sqrt{6}}$	0	$\frac{v_{dc}}{\sqrt{6}} \angle 0^\circ$
V_2	$[1,1,1,1]$	$\frac{v_{dc}}{2\sqrt{6}}$	$\frac{v_{dc}}{2\sqrt{2}}$	$\frac{v_{dc}}{\sqrt{6}} \angle 60^\circ$
V_3	$[0,1,1,1]$	$\frac{v_{dc}}{2\sqrt{6}}$	$\frac{v_{dc}}{2\sqrt{2}}$	$\frac{v_{dc}}{\sqrt{6}} \angle 120^\circ$
V_4	$[0,0,1,1]$	$-\frac{3v_{dc}}{2\sqrt{6}}$	$\frac{v_{dc}}{2\sqrt{2}}$	$\frac{v_{dc}}{\sqrt{2}} \angle 150^\circ$
V_5	$[0,0,0,1]$	$\frac{v_{dc}}{\sqrt{6}}$	0	$\frac{v_{dc}}{\sqrt{6}} \angle 180^\circ$

V_6	$[0,0,0,0]$	$-\frac{v_{dc}}{2\sqrt{6}}$	$-\frac{v_{dc}}{2\sqrt{2}}$	$\frac{v_{dc}}{\sqrt{6}} \angle 240^0$
V_7	$[0,1,0,0]$	$\frac{v_{dc}}{2\sqrt{6}}$	$-\frac{v_{dc}}{2\sqrt{2}}$	$\frac{v_{dc}}{\sqrt{6}} \angle 300^0$
V_8	$[1,1,0,0]$	$\frac{3v_{dc}}{2\sqrt{6}}$	$-\frac{v_{dc}}{2\sqrt{2}}$	$\frac{v_{dc}}{\sqrt{6}} \angle 330^0$

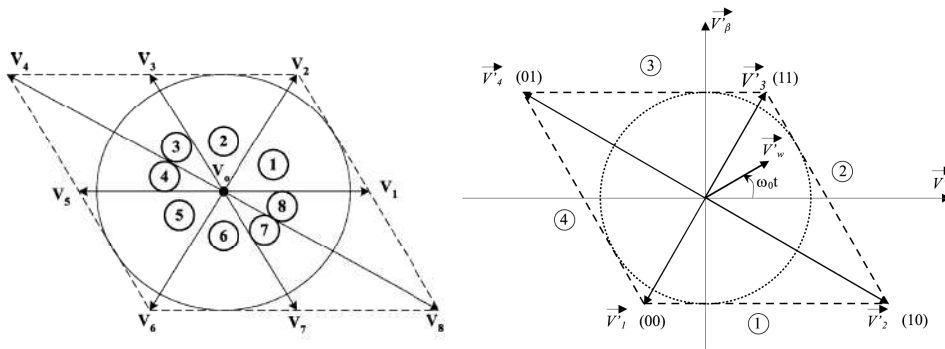


Figure 3: Space vectors and the sectors in $\alpha - \beta$ plane

Fig 3 gives the nine switching combinations and the corresponding voltage vectors in the orthogonal coordinate. There is one zero voltage vector (V_0), six small voltage vectors ($V_1, V_2, V_3, V_5, V_6, V_7$), and two large voltage vectors (V_4 and V_8). The vectors V_1 and V_5, V_2 and V_6, V_3 and V_7 are opposite in direction. The small voltage vectors have a length of $V_{dc}\sqrt{6}$ on the orthogonal coordinate plane. The other two vectors V_4 and V_8 are opposite in direction, but their vector length is $V_{dc}/\sqrt{2}$. These nine voltage vectors divide the whole circle into four sectors (sectors 1, 2, 5, and 6) with 60^0 angle duration and four sectors (sectors 3, 4, 7 and 8) with 30^0 angle duration. Fig. 3 and Table I show the definition of these sectors.

2.1 Calculation of switching times for Reference Vector

The space vector modulation and the sequencing of the selected switching vectors have been proposed in [9]–[11]. Based on the nine possible voltage vectors generated by the converter, there are eight sectors in the $\alpha\beta$ coordinate system. The reference control voltage vector V^* can be synthesized within one cycle time of length T . The reference control voltage vector V^* can be expressed as

$$V^* = m \frac{V_{dc}}{2\sqrt{2}} e^{j\theta} \tag{13}$$

Where m is a modulation index. The PWM will achieve this commanded voltage. Based on the space vector technique, the reference control voltage vector V^* can be expressed by two adjacent voltage vectors

$$V^* = V_x \frac{T_x}{T} + V_y \frac{T_y}{T} \tag{14}$$

Where T_x and T_y are time duration of voltage vectors V_x and V_y , respectively, in each sector. The time durations T_x and T_y have the following condition

$$T_x + T_y + T_o = T \tag{15}$$

Where T_0 is the time duration of voltage vector V_0 . The relationships between each sector and the corresponding two adjacent vectors to compose the reference voltage vector as given in Table 2. For example, three voltage vectors $V_1, V_2,$ and V_0 are used to compose reference voltage vector V^* in the sector 1 (0^0-60^0). The reference voltage vector V^* is synthesized by

$$\mathbf{V}^* = V_1 \frac{T_1}{T} + V_2 \frac{T_2}{T} \quad (16)$$

By projecting the control voltage vector and two adjacent vectors onto the real and imaginary parts in the α - β coordinate system, one can obtain the following relations

$$v_\alpha^* = \frac{V_{dc}}{\sqrt{6}} \frac{T_1}{T} + \frac{V_{dc}}{2\sqrt{6}} \frac{T_2}{T} \quad v_\beta^* = \frac{V_{dc}}{2\sqrt{6}} \frac{T_2}{T} \quad (17)$$

The time durations of the selected switching vectors V_1 , V_2 , and V_0 are easily calculated and expressed as

Table 2: Time Durations of the Switching Vectors in the Corresponding Sectors

S.No	Sectors	Time duration of adjustment voltage vectors		Time duration of power switches			
				T_{sa1}	T_{sa2}	T_{sb1}	T_{sb2}
1	1	$T_1 = \frac{\sqrt{6}}{V_{dc}} V_\alpha^* T - \frac{\sqrt{2}}{V_{dc}} V_\beta^* T$	$T_2 = \frac{2\sqrt{2}}{V_{dc}} V_\beta^* T$	T_1+T_2	T	T_2	T
2	2	$T_2 = \frac{\sqrt{6}}{V_{dc}} V_\alpha^* T + \frac{\sqrt{2}}{V_{dc}} V_\beta^* T$	$T_3 = -\frac{\sqrt{6}}{V_{dc}} V_\alpha^* T + \frac{2\sqrt{2}}{V_{dc}} V_\beta^* T$	T_2	T	T_2+T_3	T
3	3	$T_3 = \frac{\sqrt{6}}{V_{dc}} V_\alpha^* T + \frac{3\sqrt{2}}{V_{dc}} V_\beta^* T$	$T_4 = -\frac{\sqrt{6}}{V_{dc}} V_\alpha^* T + \frac{\sqrt{2}}{V_{dc}} V_\beta^* T$	0	T_0+T_3	T_3+T_4	T
4	4	$T_4 = \frac{2\sqrt{2}}{V_{dc}} V_\beta^* T$	$T_3 = -\frac{\sqrt{6}}{V_{dc}} V_\alpha^* T + \frac{3\sqrt{2}}{V_{dc}} V_\beta^* T$	0	0	T_4	T
5	5	$T_5 = -\frac{\sqrt{6}}{V_{dc}} V_\alpha^* T + \frac{\sqrt{2}}{V_{dc}} V_\beta^* T$	$T_6 = \frac{2\sqrt{2}}{V_{dc}} V_\beta^* T$	0	0	T_4	T_0+T
6	6	$T_6 = -\frac{\sqrt{6}}{V_{dc}} V_\alpha^* T - \frac{\sqrt{2}}{V_{dc}} V_\beta^* T$	$T_7 = \frac{\sqrt{6}}{V_{dc}} V_\alpha^* T - \frac{\sqrt{2}}{V_{dc}} V_\beta^* T$	0	T_0+T_7	0	T_0
7	7	$T_7 = -\frac{\sqrt{6}}{V_{dc}} V_\alpha^* T - \frac{3\sqrt{2}}{V_{dc}} V_\beta^* T$	$T_8 = \frac{\sqrt{6}}{V_{dc}} V_\alpha^* T + \frac{\sqrt{2}}{V_{dc}} V_\beta^* T$	T_8	T	0	T_0
8	8	$T_8 = \frac{2\sqrt{2}}{V_{dc}} V_\beta^* T$	$T_1 = -\frac{\sqrt{6}}{V_{dc}} V_\alpha^* T + \frac{2\sqrt{2}}{V_{dc}} V_\beta^* T$	T_8+T_1	T	0	T_0+T_1

Sequencing of power switches within one switching period T

Table2 give the sequencing of the power switches in sectors 2–8, respectively. The reference voltage vector \mathbf{V}^* can be composed to control the line currents with unity power factor. In the conventional space vector modulation, the magnitude and phase angle of the reference voltage vector must be given to determine the sector location and to calculate the time duration of adjacent vectors. This control algorithm is so complicated that it requires a long computation time. To reduce the computation time of trigonometric function and square root operation in (7), four lines are defined to divide the whole circle into eight sectors. These four lines are

$$\begin{aligned} P_1 : y = 0, P_2 : y = \sqrt{3}x \\ P : y = -\sqrt{3}x, P_4 : y = -x/\sqrt{3} \end{aligned} \quad (18)$$

Therefore, any point of reference voltage vector V^* in the orthogonal coordinate system can determine its location through these four equations in (18). Table 3 and Fig. 4 give the relationships between the sector where the reference voltage vector V^* lies in and the values of variables P1–P4.

TABLE 3: RELATIONSHIP BETWEEN SECTOR WHERE REFERENCE VECTOR LIES AND P1-P2

Sector	1	2	3	4	5	6	7	8
P1	1	1	1	1	0	0	0	0
P2	0	1	1	1	1	0	0	0
P3	1	1	0	0	0	0	1	1
P4	1	1	1	0	0	0	0	1
P1, P1, P1, P1	(1,0,1,1)	(1,1,1,1)	(1,1,0,1)	(1,1,0,0)	(0,1,0,0)	(0,0,0,0)	(0,0,1,0)	(0,0,1,1)

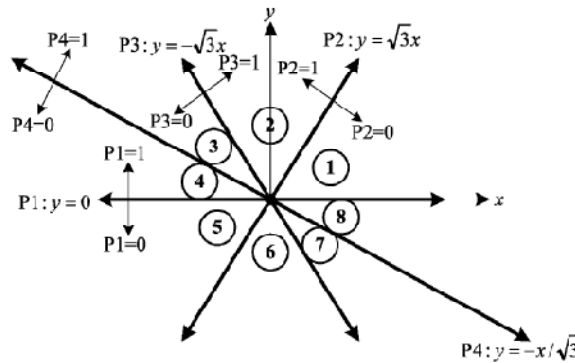


Figure 4: Relationship between sector where reference vector lies and P1-P4

Variables P1–P4 are defined as

$$\begin{aligned}
 v_\beta &\geq 0 (p_1 = 1) \quad v_\beta < 0 (p_1 = 0) \\
 v_\beta &\geq \sqrt{3}v_\alpha (p_2 = 1) \quad v_\beta < \sqrt{3}v_\alpha (p_2 = 0) \\
 v_\beta &\geq \sqrt{3}v_\alpha (p_3 = 1) \quad v_\beta < -\sqrt{3}v_\alpha (p_3 = 0) \\
 v_\beta &\geq -v_\alpha/\sqrt{3} (p_4 = 1) \quad v_\beta < -v_\alpha/\sqrt{3} (p_4 = 0)
 \end{aligned} \tag{19}$$

Now we can use variables P1–P4 to determine the sector where reference vector V^* lies in and to calculate the time duration of power switches. No calculation of trigonometric function and square root operation is needed in the adopted algorithm.

2.2 Proposed Controller Control Block

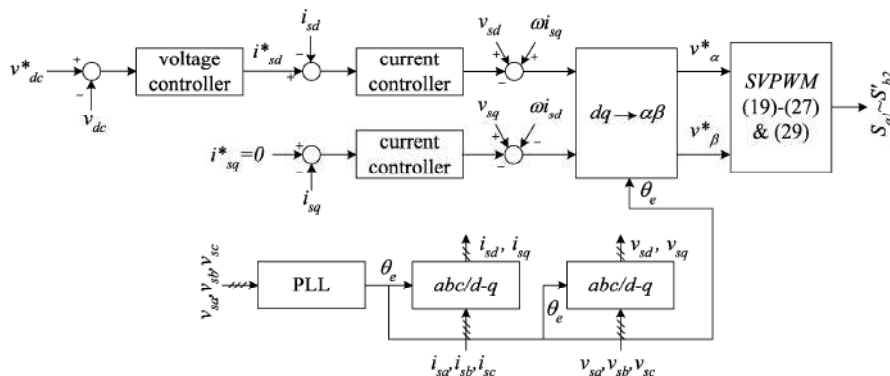


Figure 5: Block diagram of the proposed control algorithm

Fig. 5 give the control block of the proposed control algorithm. A dc bus voltage controller is used to balance the power demand between the ac source and dc load. A current controller is used to obtain the reference control voltage vector of the converter. The simplified space vector modulation is adopted to obtain the time duration of the selected voltage vectors. The time intervals of power switches corresponding to the selected voltage vectors are calculated to drive the converter. The control goals of the proposed converter are to obtain a constant dc-link voltage, to draw the sinusoidal line currents, and to achieve unity input power factor.

The algorithm of the closed-loop compensators in the synchronous reference frame is used in the control scheme. A voltage controller is adopted to obtain the line current command i_{sd}^* .

For a unity power factor operation, the line current command i_{sq}^* is set to zero. The reference voltage vector V_e in the synchronous reference frame can be obtained by the transformation from α - β coordinate system to synchronous reference frame

$$V^e = V_s^e - rI_s^e - L \frac{dI_s^e}{dt} - j\omega L I_s^e \quad (20)$$

where

$$\begin{aligned} I_s^e &= \begin{pmatrix} i_{sd} \\ i_{sq} \end{pmatrix} = T \begin{pmatrix} i_{s\alpha} \\ i_{s\beta} \end{pmatrix} & V_s^e &= \begin{pmatrix} v_{sd} \\ v_{sq} \end{pmatrix} = T \begin{pmatrix} v_{s\alpha} \\ v_{s\beta} \end{pmatrix} \\ V^e &= \begin{bmatrix} v_d \\ v_q \end{bmatrix} = T \begin{pmatrix} v_\alpha \\ v_\beta \end{pmatrix} & T &= \begin{pmatrix} \cos \theta & \sin \theta \\ -\sin \theta & \cos \theta \end{pmatrix} \end{aligned} \quad (21)$$

If the voltage drop on the resistor r can be neglected, then the reference voltage on the ac terminal in the synchronous reference frame is expressed as

$$v_d \approx v_{sd} - L \frac{di_{sd}}{dt} + \omega i_{sq} \quad (22)$$

$$v_q \approx v_{sq} - L \frac{di_{sq}}{dt} + \omega i_{sd} \quad (23)$$

Three-phase line currents are measured and transformed into the synchronous reference frame. Based on (22) and (23), the voltage command on the ac terminal in the synchronous reference frame are calculated. Using the coordinate transformation from the synchronous reference frame into the stationary reference frame, the voltage commands v_α^* and v_β^* are achieved. The sector where the reference voltage vector lies in can be obtained based on the values of P1–P4. Two adjacent vectors and the time duration of power switches in each sector can be calculated. The sequencing of power switches shown in Table 2 is exported to the gate drive circuits. The reference voltage vector V^* can be composed by the properly two voltage vectors in each sector

3. SIMULATION RESULTS

3.1 Simulation Parameters

Some simulation is presented to confirm the validity and effectiveness of the proposed control scheme. Simulation was performed in the SIMULINK toolbox of MATLAB. The power stage parameters of the three-phase converter are

Dc link capacitance: 2200 μ F, Power switches: IGBT IRG4PC40W, Boost inductor: 5 mH, Switching frequency: 20 kHz, The line voltage is :110 V, source frequency : 60 Hz, The dc link voltage equals: 400 V, Resistive Load R :20 ohms, R-L Load, R=15 ohms, L=5mH

3.2 Simulation Outputs

For R Load, simulated results of power factor with controller are shown in Fig 8 and without controller is shown in Fig. 8 Simulated results of AC terminal voltages for $V_0=400$ V are shown in Fig 9. Simulated results of capacitor voltages for $V_0=400$, $V_0=500$ and $V_0=600$ are shown in Fig 9. Simulated results of values P1 to P4 are shown in Fig 10. The required gate pulses for power switches are shown in Fig 11.

For R-L Load, simulated results of power factor with controller are shown in Fig 12. Simulated results of AC terminal voltages for $V_0=400$ V are shown in Fig 12. Simulated results of capacitor voltages for $V_0=400$ and DC Motor Load

For R Load

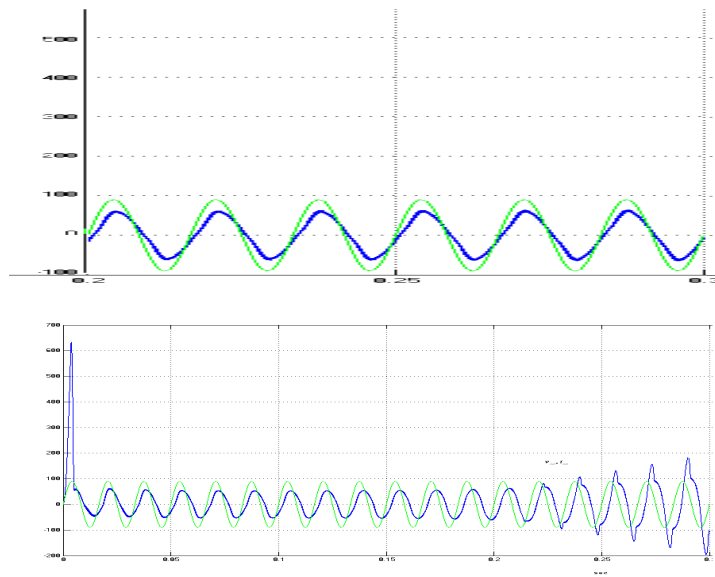


Figure 6: Power Factor with controller & Power Factor without controller

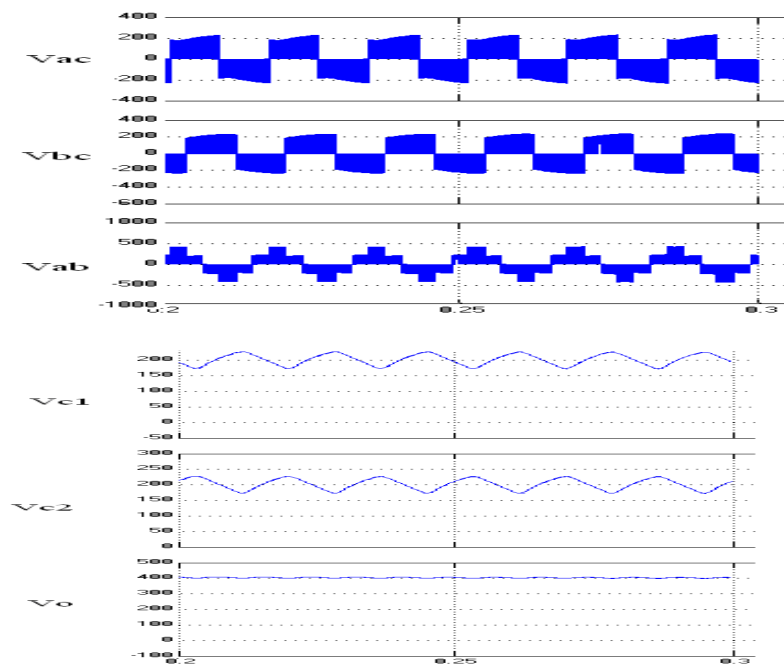
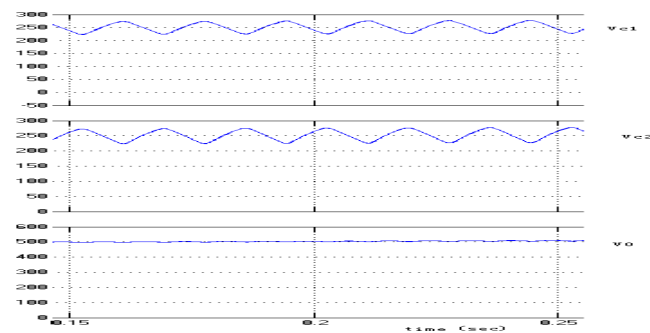


Figure 7: AC Terminal Voltages & Simulated Capacitor Voltages for $V_o = 400V$



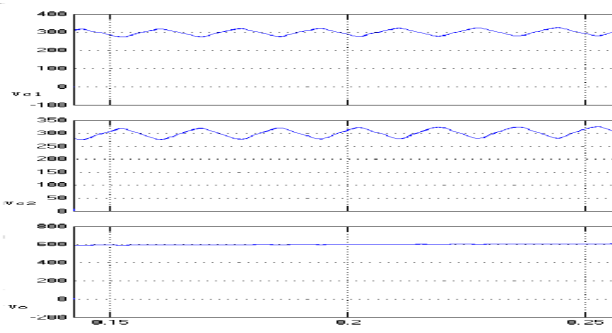


Figure 8: Simulated Capacitor Voltages for $V_o=500V$ & $V_o=600V$

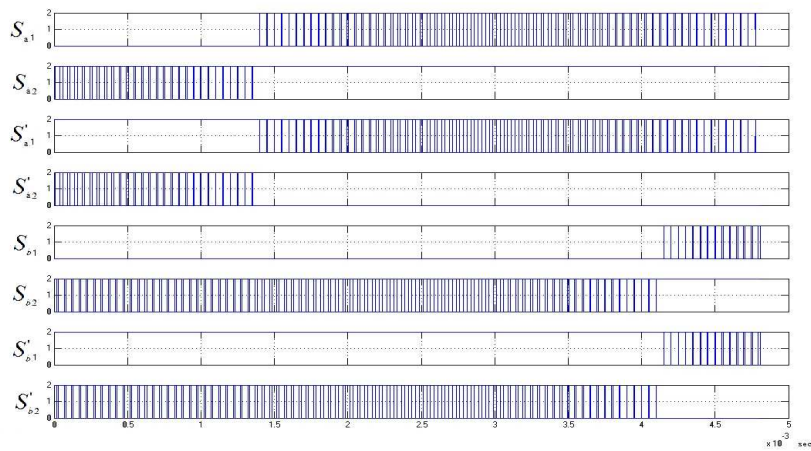
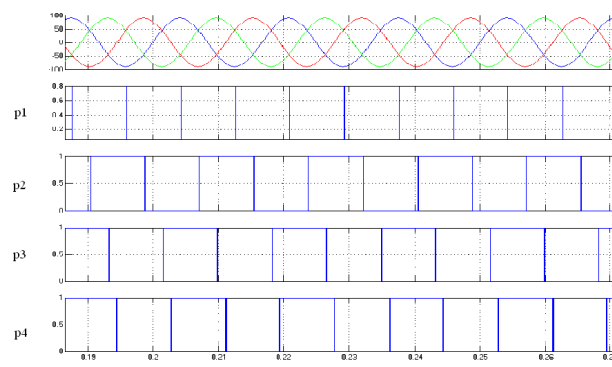


Figure 8: P1-P4 simulated results & Switching signals of power switches

For RL Load

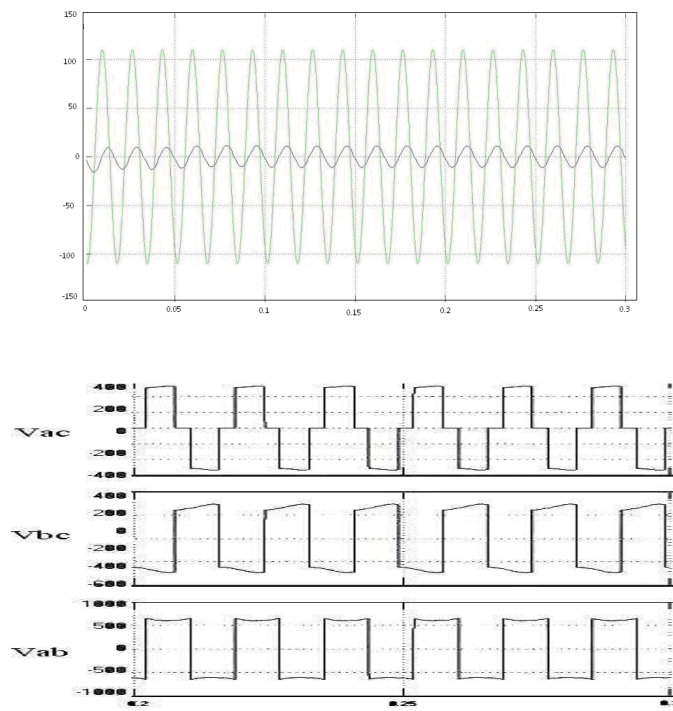


Figure 9: Power Factor with controller & AC Terminal Voltages

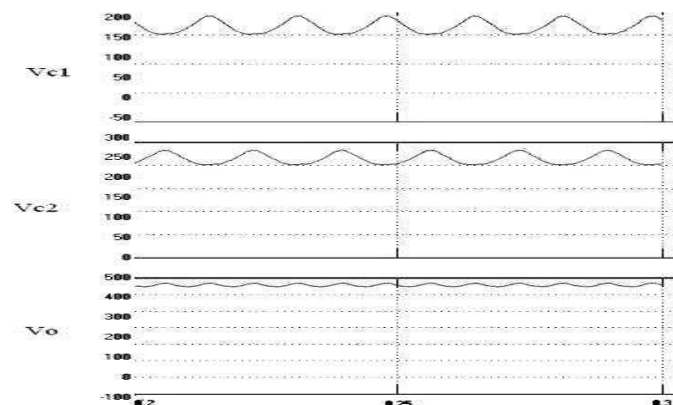


Figure 9: Simulated Capacitor Voltages for $V_o=500V$

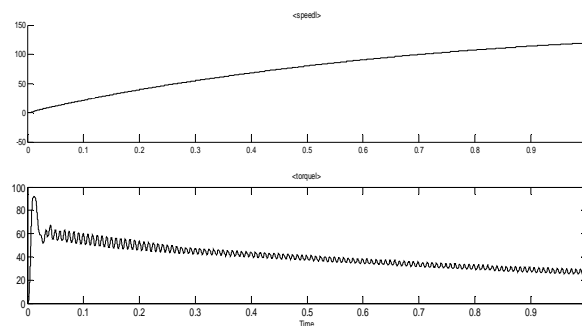


Figure 10: Simulated Speed and Torque outputs of Dc motor

4. CONCLUSIONS

A simple PWM scheme based on space vector modulation for an eight-switch three-phase NPC converter is presented to save the calculation time, to obtain the time duration of power switches, and to control the line currents with unity input power factor. The circuit configuration is simple compared with the conventional twelve-switch three-phase NPC converter. Only eight power switches and four clamping diodes are used in the converter.

In the proposed converter, the dc bus voltage is greater than two times of line voltage ($V_{dc} > 2V_{line}$). The size of capacitor in the proposed converter is twice larger than that in the conventional twelve switches NPC converter to maintain the same voltage ripple. With the proposed control scheme, the sinusoidal line currents with unity power factor drawn from the ac source and constant dc-link voltage are achieved. Computer simulation results are presented to demonstrate the validity and effectiveness of the proposed control scheme.

REFERENCES

- [1] Bor-Ren Lin, Ta-Chang Wei, "Space vector modulation strategy for an Eight-switch three-phase NPC converter" *IEEE Transactions on Aerospace and electronic systems*, vol. 40, NO.2, April 2004.
- [2] Dallago, E., Sasone, G., Storti, M., and Venchi, G. (1998) Experimental analysis and comparison on a power factor controller including a delta-sigma processing stage. *IEEE Transactions on Industrial Electronics*, 45, 4 (1998), 544–551.
- [3] Zheren Lai, and Smedley, K. M. (1998) A family of continuous-conduction-mode power-factor-correction controllers based on the general pulse-width modulator. *IEEE Transactions on Power Electronics*, 13, 3 (1998), 501–510.
- [4] Hirachi, K., and Nakaoka, M. (1999) Novel PFC converter suitable for engine-driven generator-interactive three-phase power systems. *IEE Proceedings—Electric Power Applications*, 146, 2 (1999), 253–260.
- [5] Qiao, C., and Smedley, K. M. (2002) A general three-phase PFC controller for rectifiers with a parallel-connected dual boost topology. *IEEE Transactions on Power Electronics*, 17, 6 (2002), 925–934.
- [6] Hahn, J., Enjeti, P. N., and Pitel, I. J. (2002) A new three-phase power-factor correction (PFC) scheme using two single-phase PFC modules. *IEEE Transactions on Industry Applications*, 38, 1 (2002), 123–130.
- [7] Konishi, Y., and Nakaoka, M. (1998) Current-fed three-phase converter with optimum PWM scheme and its practical input line filter design. *IEE Proceedings—Electric Power Applications*, 145, 6 (1998), 535–543.
- [8] Mwinyiwiwa, B., Wolanski, Z., and Ooi, B-T. (1998) Microprocessor-implemented SPWM for multiconverters with phase-shifted triangle carriers. *IEEE Transactions on Industry Applications*, 34, 3 (1998), 487–494.
- [9] Dai, S-Z., Lujara, N., and Ooi, B-T. (1992) A unity power factor current-regulated SPWM rectifier with a notch feedback for stabilization and active filtering. *IEEE Transactions on Power Electronics*, 7, 2 (1992), 356–363.
- [10] Trzynadlowski, A. (1996) An overview of modern PWM techniques for three-phase, voltage-controlled, voltage source inverters. In *Proceedings of the International Symposium Industry Electronics Conference*, Warsaw, Poland, 1996, 25–39.
- [11] Holtz, J. (1996) Pulsewidth modulation—A survey. *IEEE Transactions on Industrial Electronics*, 39, 6 (1996), 410–420.
- [12] Kzamierekowski, M. P., and Dzieciakowski, M. A. (1994) Review of current regulation techniques for three-phase PWM inverters. In *Proceedings of the International Symposium Industry Electronics Conference*, Bologna, Italy, 1994.
- [13] Nabea, A., Takahashi, I., and Akagi, H. (1981) A new neutral-point clamped PWM inverter. *IEEE Transactions on Industry Applications*, 17, 5 (1981), 518–523.
- [14] Lai, J. S., and Peng, F. Z. (1996) Multilevel converters—A new breed of power converter. *IEEE Transactions on Industry Applications*, 32, 3 (1996), 509–517.
- [15] Meynard, T., and Foch, H. (1993) Imbricated cells multilevel voltage source inverters for high voltage applications. *EPE Journal*, 3, 2 (1993), 99–106.
- [17] Lee, S-G., Kang, D-W., Lee, Y-H., and Hyun, D-S. (2001) The carrier-based PWM method for voltage balance of flying capacitor multilevel inverter. In *Conference Record of IEEE-PESC*, 2001, 126–131.
- [18] Peng, F. Z., Lai, J. S., Mckeever, J. W., and Vancoevering, J. (1996) A multilevel voltage-source inverter with separate dc sources for static VAR generation. *IEEE Transactions on Industry Application*, 32, 5 (1996), 1130–1137.
- [19] Manjrekar, M. D., Steimer, P. K., and Lipo, T. A. (2000) Hybrid multilevel power conversion system: a competitive solution for high-power applications. *IEEE Transactions on Industry Application*, 36, 3 (2000), 834–841.
- [20] Pou, J., Boroyevich, D., and Pindado R. (2002) New feed forward Space Vector PWM method to obtain balanced A.C output voltages in a three-level neutral point-clamped converter *IEEE Transactions on Industrial Electronics* 49.5(2002), 1026-1034.
- [21] Sinha, G., and Lipo, T. A. (1995) A four level rectifier-inverter system for drive applications. In *Conference Record of IEEE-IAS Annual Meeting*, 1995, 980–987.
- [22] Zhao, Y., Li, Y., and Lipo, T. A. (1995) Force commutated three level boost type rectifier. *IEEE Transactions on Industry Applications*, 31, 1 (1995), 155–161.
- [23] Salmon, J.C.: 'Techniques for minimizing the input current distortion of current-controlled single-phase boost rectifier', *IEEE Trans. Power Electron.*, 1993, 8, (4), pp. 509–520

- [24] Salmon, J.C.: 'Circuit topologies for single-phase voltage doubler boost rectifier', IEEE Trans. Power Electron., 1993, 8, (4), pp. 521–529
- [25] Manias, S.: 'Novel full-bridge semi controlled switch mode rectifier', IEE Proc. B, 1991, 138, (5), pp. 252–256
- [26] Martinez, R., and Enjeti, P.N.: 'A high-performance single-phase rectifier with input power factor correction', IEEE Trans. Power Electron., 1996, 11, (2), pp. 311–317
- [27] Wong, C., Mohan, N., and He, J.: 'Adaptive phase control for three phase PWM AC to DC converters with constant switching frequency'. Proc. Conf. PCC-Yokohama, Yokohama, Japan, 1993, pp. 73–78

BIOGRAPHY OF AUTHORS



B. Sirisha obtained her B.E degree in Electrical & Electronics Engineering from Osmania University and M.E degree in 2003 from JNTU, Hyderabad. She is currently working as Assistant Professor in Department of Electrical Engineering, University College of Engineering(Autonomous), Osmania University, Hyderabad, Andhra Pradesh, India. Her research interests include Power Electronics and Power Quality.



N. Susheela obtained her B.Tech degree in Electrical & Electronics Engineering in 2003 from SSJ Engineering College, JNTU and M.E degree in 2009 in Electrical Engineering from Osmania University, Hyderabad. She is currently working as Assistant Professor in Department of Electrical Engineering, University College of Engineering(Autonomous), Osmania University, Hyderabad, Andhra Pradesh, India. Her research interests include Power Electronics and Industrial Drives.



Dr. P. Satish Kumar was born in Karimnagar, Andhra Pradesh, INDIA in 1974. He obtained the B.Tech degree in electrical engineering from JNTU College of Engineering, Kakinada in 1996. He obtained M.Tech degree in power electronics in 2003 and Ph.D. in 2011 from JNTUH, Hyderabad. He has more than 16 years of teaching and research experience and presently working as Senior Assistant Professor in the Department of Electrical Engineering, University College of Engineering, Osmania University, Hyderabad, INDIA. He presented many research papers in various national and international journals and conferences. His research interests include Power Electronics Drives, Multilevel inverters, Matrix Converters and special Machines.